Egypt.J.Chem. **Vol. 63**, No. 6. pp. 2009 - 2018 (2020)

Egyptian Journal of Chemistry
http://ejchem.journals.ekb.eg/

Structural and Vibrational Properties of ZnSe Nanostructures: A DFT/TDDFT Study

Hussein H. Abed[1*], Mohammed J. Alsultani[2], Muder A. Abdulsattar[3], Hayder M. Abduljalil[1]

[1] *Department of Physics, College of Science, University of Babylon, Iraq.*
[2] *Environmental Health Department, College of Environmental Sciences, AL-Qasim Green University, Iraq.*
[3] *Ministry of Science and Technology, Baghdad, Iraq.*

THE structural and vibrational properties of Zn_nSe_n (n=1,3,7,13) nanostructures have been investigated using the Gaussian 09 program, density functional theory (DFT) and time-dependent density functional theory (TDDFT) at the B3LYP level with 6–311G basis functions. The structural properties showed that the rebuilding in surface atoms deviated many bonds from their ideal length, the Zn-Se bond length decreased with the increase in the size of nanostructures and converged to the experimental value. Quantum confinement effect diminution was observed with the growing size of the nanostructures; hence, the energy gap converged to the experimental value of 2.7 eV. Moreover, the binding energy increased with the increase of the structure size, such that wurtziod2c ($Zn_{13}Se_{13}$) is more stable than smaller structures. The vibrational properties results indicated that the experimental longitudinal optical mode (LO mode) is situated between bare and hydrogen passivated LO modes and very near to the bare case, this gave a good agreement with experimental findings. The presence of hydrogen atoms at the surface caused a several times decrease in vibrational force constant in comparison to the bare case. The IR spectrum for wurtzoid and HP wurtzoid were investigated. The optical edge in UV-Vis spectra of wurtzoid reduced from 4.5 eV to 4.2 eV of wurtzoid2c due to the increase in the size of the nanostructure, while the maximum peak for wurtzoid at 2.88 eV increased to 3.06 eV for wurtzoid2c showing a clear blue shift. These results leads to wide applications in fields such as photoelectronic devices, lasers, sensors, and LEDs.

Keywords: Wurtzoids, DFT/TDDFT, Nanocrystals.

Introduction

Nanostructures of semiconducting materials with a given size and composition can be synthesized nowadays generating a wide interest in investigating these structures in order to discover new technologies and applications [1-3]. Physicochemical properties for nanomaterial depend on the size and shape of nanostructures which are different from their bulk form characteristics [4]. Hence, in order to study the such structures at their nanosize level, a molecular species representing the unit cell are required to build the nanostructure of materials. Nanostructures have significant applications [5-14] which required extensive theoretical and experimental studies of different promising materials. It has been observed that quantized and surface effects are dominant parameters at nanostructures level. Fortunately, it is possible to modify these nanostructures to create them with the desired properties. Nanostructures of II-VI semiconductors have interesting characteristics; they have a wide energy gap, bright photoluminescence, high stability, and

*Corrresponding author e-mail: hakimhussein.2017@gmail.com; sci. hussein. hakim@uobabylon.edu. iq
Tel:+9647804078871
Received 24/7/2019; Accepted 21/11/2019
DOI: 10.21608/ejchem.2019.15190.1922
©2020 National Information and Documentation Center (NIDOC)

size dependence. Therefore, they are used in different applications such as LEDs, solar cells, sensors, biological photoelectrochemical cells, and catalysts [15-18]. Zinc selenide (ZnSe) is an II-VI compound having a direct bandgap of 2.7 eV. ZnSe is recognized to be a favorable material for red, blue and green LEDs, photodetectors, transistors, photoelectrochemical cells, inorganic semiconductor for core/shell, and doped nanocrystals, etc. [19,20]. ZnSe at nanoscale exhibitions incredibly different properties than bulk form. In this work, wurtzoids will be used to represent the wurtzite at the nanoscale in order to investigate the structural and vibrational properties of ZnSe. As such, the nanostructures Zn_nSe_n where n is the number of atoms (n=1,3,7,13) will be considered.

Models and Method

Wurtzite and diamond structure at molecular and nanoscale regimes can be represented by a small molecule called wurtzoid and diamondoid, respectively [21-24]. The surface atoms of these molecules are usually passivated with hydrogen or other atoms to saturate the dangling bond and make bulk wurtzite and diamond crystals. If not passivated, these unsaturated atoms tend to reorganize and undergo a surface reconstruction to minimize the surface energy. Wurtzoids are the building blocks of the wurtzite structure. As in the wurtzite structure, a and c parameters are needed to describe wurtzoids, i.e., these wurtzoids are cupped bundles of (3,0) nanotubes of ZnSe. Fig. 1 shows the smallest CdSe molecules in the wurtzite structure is wurtzoid (Zn_7Se_7) and wurtzoid2c ($Zn_{13}Se_{13}$) after geometrical optimization. Fig. 1 also shows ZnSe diatomic molecule and ZnSe bare cyclohexane (Zn_3Se_3), these two molecules are also the component building block of both wurtzoids and diamondoids. Hydrogen passivated wurtzoid (HP wurtzoid) also shown in Fig.1. All the clusters in Fig. 1 are geometrically optimized using the Gaussian 09 program, density functional theory and time-dependent density functional theory at the B3LYP level with 6–311G basis functions[25]. UV-vis spectrum was calculated using time-dependent density functional theory.

Results and Discussions

Density of bonds

Three kinds of bonds exist in bare and HP wurtzoid. These are Zn-H, Se-H, and Zn-Se. The shortest bonds are Zn-H bonds followed by Se-H bonds. The widest distribution of bond lengths is in Zn-Se bonds. The reconstruction in surface calculations deviates many bonds from their ideal length. Fig. 2 show the distribution of bond lengths of bare wurtzoid, HP wurtzoid, and bare wurtzoid2c. The Zn–Se average bond lengths are 2.54 Å in the bare wurtzoid, 2.7Å in the HP wurtzoid and 2.52 Å for wurtzoid2c. It is in a good agreement with experimental value 2.45Å [26]. The bond length decreases with increasing the size of the molecule. This result agrees with the experimental measurement [18]. Se–H and Zn–H bond lengths are 1.475 Å and 1.54 Å, respectively, Zn and Se atoms are attached to hydrogen atoms to saturate dangling bonds.

Energy gap and binding energy

The variation of the energy gap of bare ZnSe structures is shown in Fig. 3. The Figure shows that ZnSe structures tend to converge to the bulk experimental gap. ZnSe structures obey quantum confinement rule of approaching the bulk energy gap with the increase of the structure size. However, due to a large number of dangling bonds in both ZnSe and Zn_3Se_3 molecules for the actual number of bonds of the two molecules, the energy gap is decreased since the dangling bonds create energy levels inside the original energy gap that decreases its value as shown in Table 1. As the molecules increase in size, the number of dangling bonds decreases for the total number of bonds that prevents gap reduction and renders quantum confinement rule of approaching bulk energy gap [24].

The binding energy is calculated by using the relation:

E_binding=((nZn+nSe)-Zn_n

Where n is number of atoms.

Fig. 4 shows the variation of binding energy with the number of atoms. The binding energy increases with the increased size of the structure. The wurtzoid2c is more stable than other structures because it has high binding energy. The dangling bonds decreased with the increased size of structures and causes a rise in the binding energy as shown in Table 1.

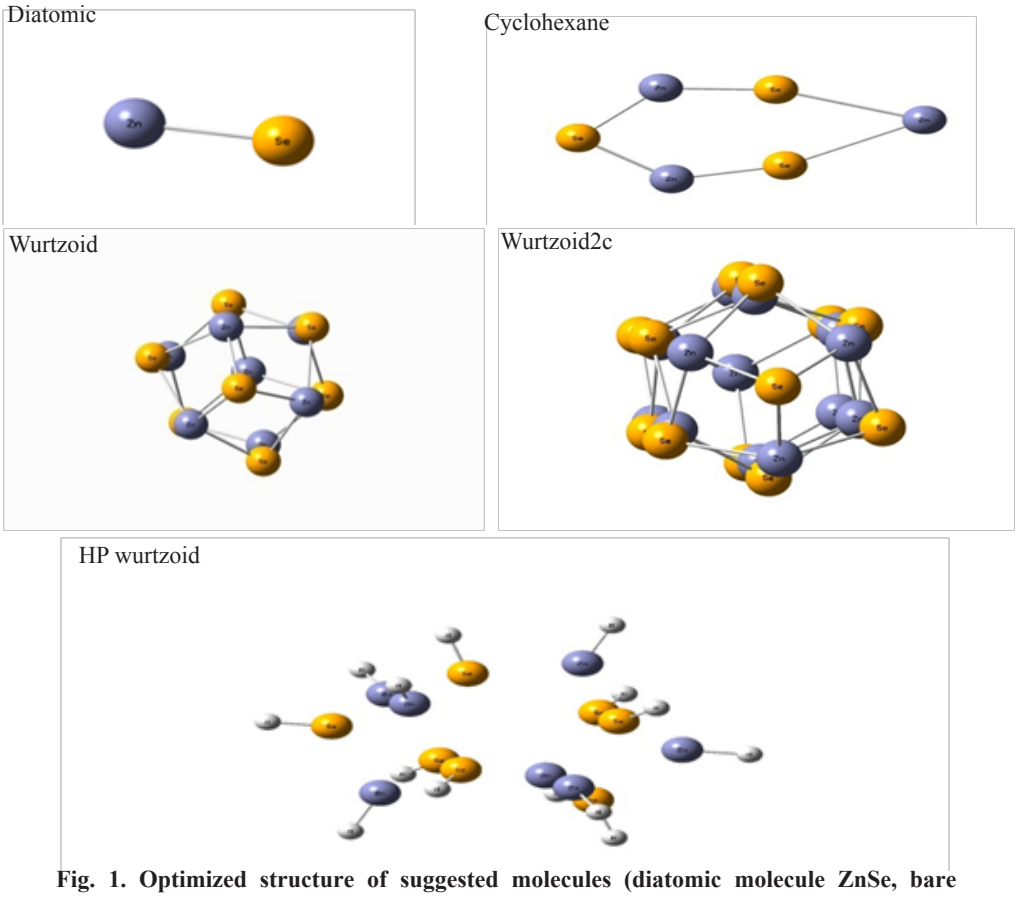

Fig. 1. Optimized structure of suggested molecules (diatomic molecule ZnSe, bare cyclohexane Zn_3Se_3, bare wurtzoid Zn_7Se_7, bare wurtzoid2c $Zn_{13}Se_{13}$, and hydrogen passivated wurtzoid $Zn_7Se_7H_{14}$).

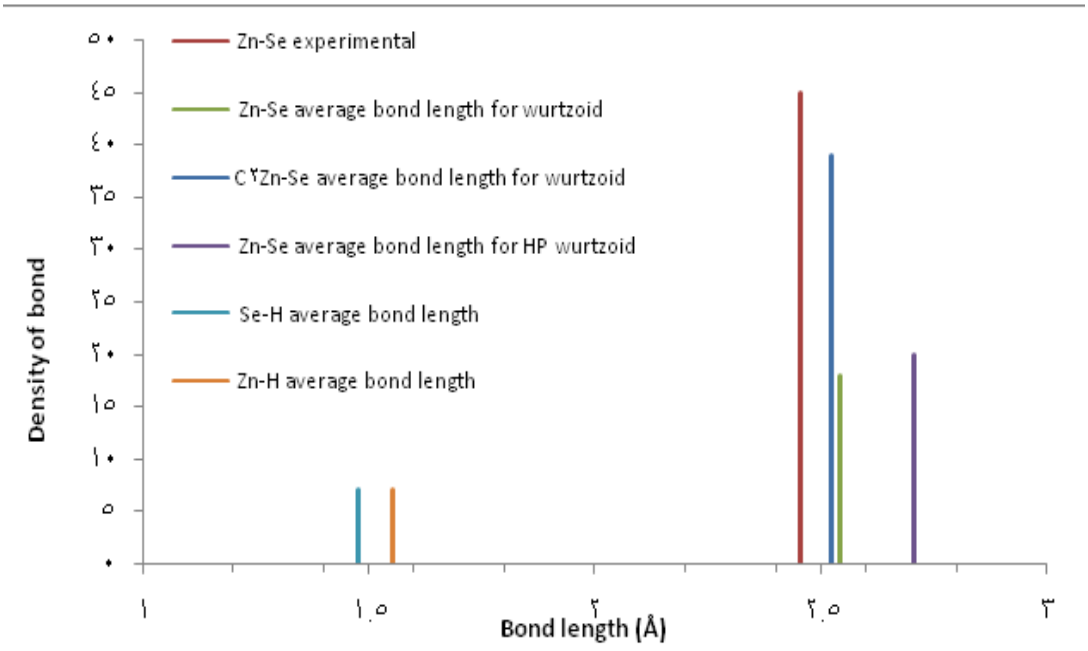

Fig. 2. Average bond length (Å) for wurtzoid, wurtzoid2c, and HP wurtzoid.

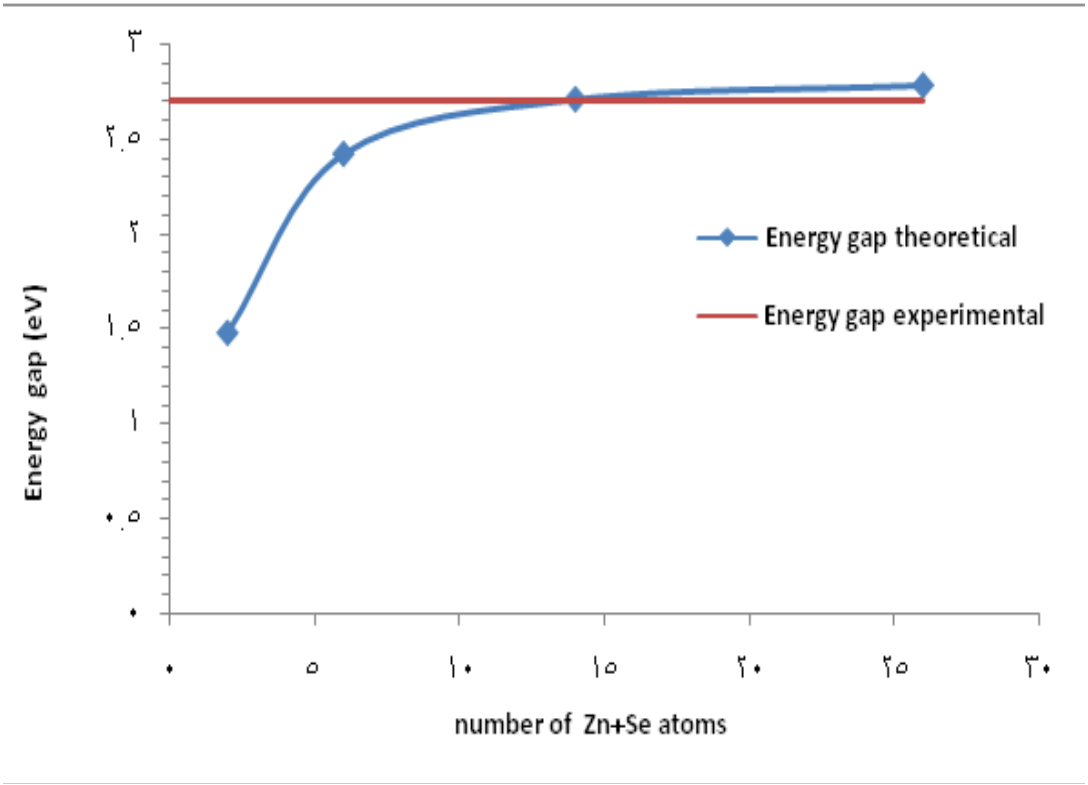

Fig. 3. The variation of the energy gap of bare ZnSe structures.

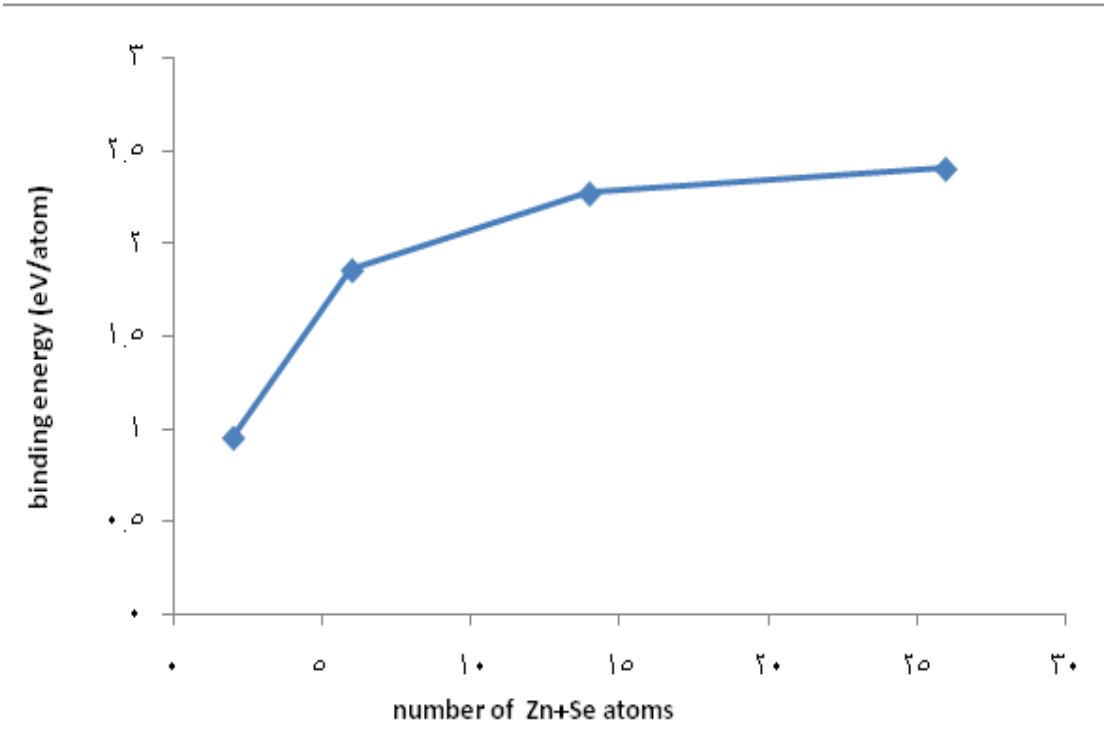

Fig. 4. Binding energy of bare ZnSe structures.

TABLE 1. Energy gap and binding energy for the structures.

Structures	Energy gap eV	Energy gap experimental eV	Binding energy eV/atom
ZnSe Diatomic	1.478		0.952
Zn_3Se_3 Cyclohexane 2.425			1.859
Zn_7Se_7 Wurtzoid	2.714	2.7	2.274
$Zn_{13}Se_{13}$ Wurtzoid2c	2.788		2.407

Reduced mass and force constant

Fig. 5 shows the variation of reduced mass as a function of the frequency of bare wurtzoid and HP wurtzoid. The longitudinal optical mode (LO) can be deduced from this figure. The LO mode is the last vibrational mode in the bare case. In the same way, the LO mode is the last vibrational mode in the HP case before the beginning of the hydrogen vibrations. The hydrogen vibrations are characterized by a reduced mass that is nearly equal to 1. LO modes of both bare and HP wurtzoids, which are shown in Fig. 5 in comparison with experimental LO value at 250 cm^{-1} [10,26]. Also, from Fig. 5, it can be seen that the experimental LO mode is situated between bare and HP LO modes and very near to the bare case, this phenomenon can be correlated with Fig. 2 that shows the weak bonding between surface hydrogenated atoms and the rest of the molecule. Surface hydrogen atoms are easily removed so that these molecules are partially hydrogenated in real experiments.

The vibrational force constant shown in Fig. 6, which in its bare mode is several times higher than that of the HP case. The surface dangling bonds are the cause of this large increase. The electronic charge of dangling bonds strengthens other real bonds so that nearly double bonds are created in other bonds. Various hydrogen vibrations can be seen in the HP case in addition to the Zn-Se vibrations discussed previously and shown in Fig. 1. Se-H and Zn-H bending vibrations can be seen in the range 288-556 cm^{-1}. These bending vibrations are followed by an island of Se-H stretches at the range 1824-1850 cm^{-1}. Finally, an island of Zn-H stretching can be seen at the range of 2297-2339 cm^{-1}.

IR Spectrum

Fig. 7 shows the IR spectrum of ZnSe wurtzoid structure molecule. IR spectrum for wurtzoid has two high peaks; one at 208.8 cm^{-1} and another at 252.6 cm^{-1}. Fig. 8 shows the IR spectrum of HP wurtzoid structure molecule. The IR spectrum for HP wurtzoid can be divided into four regions depending on the properties of vibration. In the first region, pure Zn-Se vibrations results have shown a good matching to the experimental measurement [10,26]. The second region, Se-H and Zn-H bending vibrations. In the third region, Se-H stretching has a high peak at 1612 cm^{-1}. The fourth region Se-H stretching has lower intensity when compared with the three above mentioned regions for HP wurtzoid.

UV-vis Spectrum

UV-vis spectra of wurtzoid and wurtzoid2c are shown in Fig. 9. The optical edge in UV-vis spectra moves from 275.4 nm for wurtzoid to 295.2 nm for wurtzoid2c, this reduction (redshift) in excitation energy from 4.5 eV to 4.2 eV is due to the increase in the size of the molecule. In the molecular and nanoscale regime, the number of atoms and also atomic orbitals involved in the overlap are much smaller than the bulk counterpart which causes an increase of the optical band gap at the nanoscale. The maximum peak for wurtzoid at 430.2 nm and wurtzoid2c at 405 nm which shows a clear blue shift. Fig. 9 shows that the width of the UV-vis peak for wurtzoid is wider in comparison to the nanostructure case while its amplitude is lower where the amplitude of the nanostructure case is much sharper. This means that the optical behavior for ZnSe nanostructure can be changed by changing the size of the nanostructure. This result leads to wide applications such as in photoelectronic devices, lasers, sensors, and LEDs.

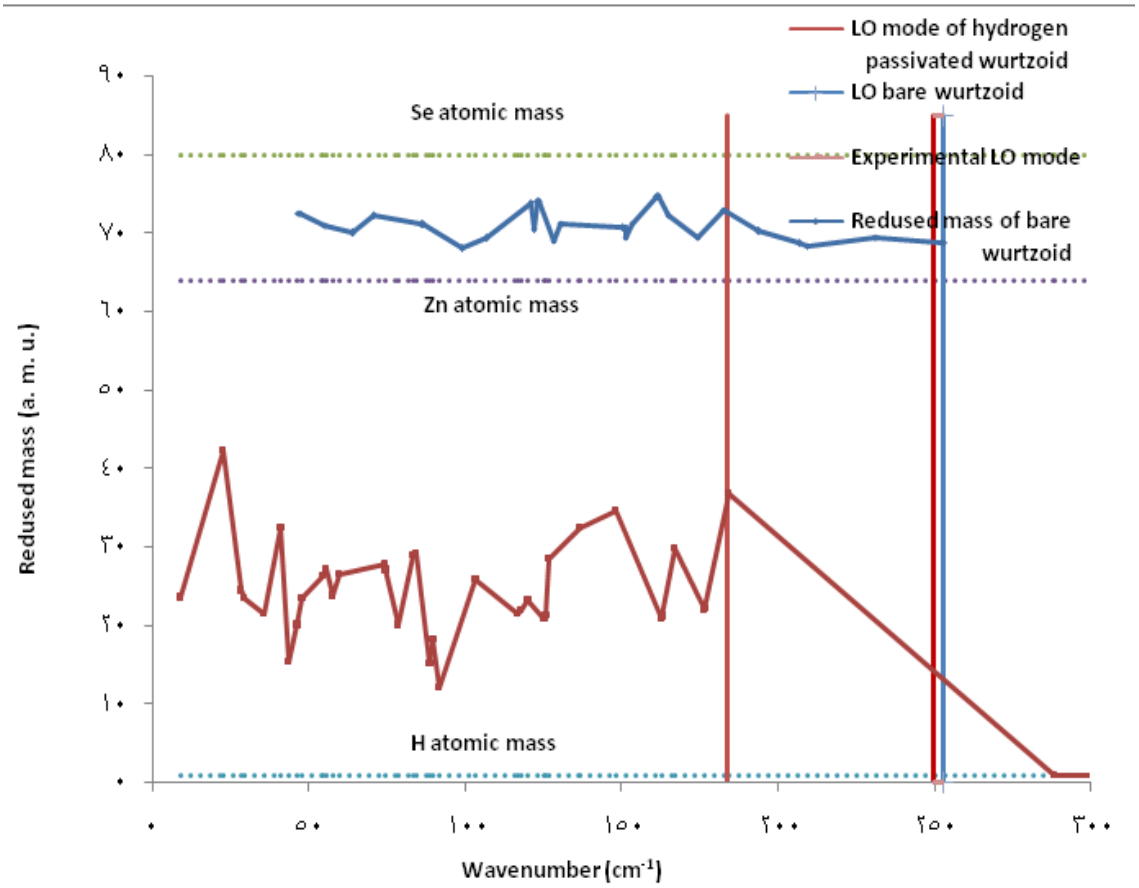

Fig. 5. Vibrational reduced mass for bare wurtzoid and HP wurtzoid

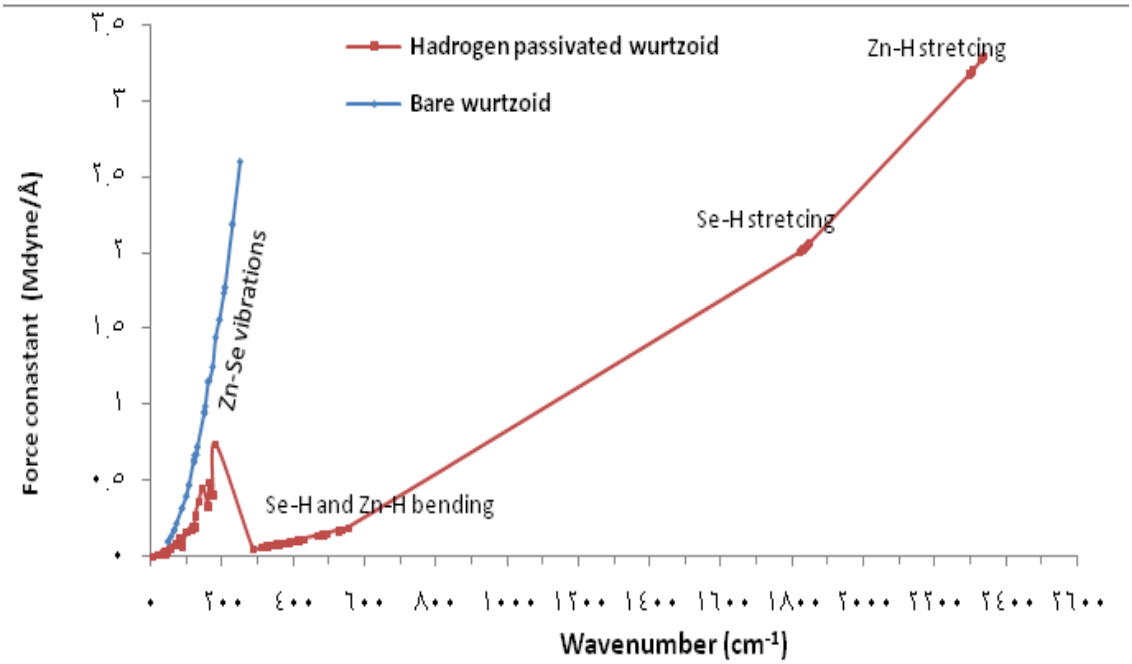

Fig. 6. Vibrational force constant for bare wurtzoid and HP wurtzoid.

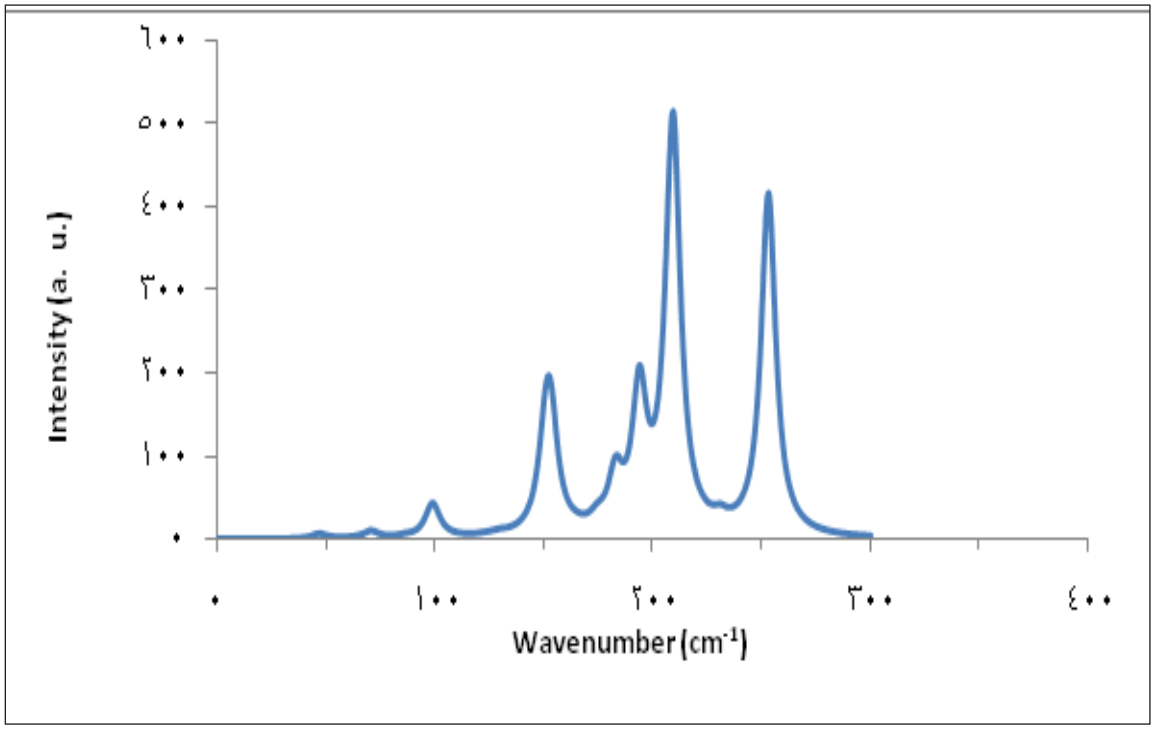

Fig. 7. IR spectrum of ZnSe wurtzoid structure molecules.

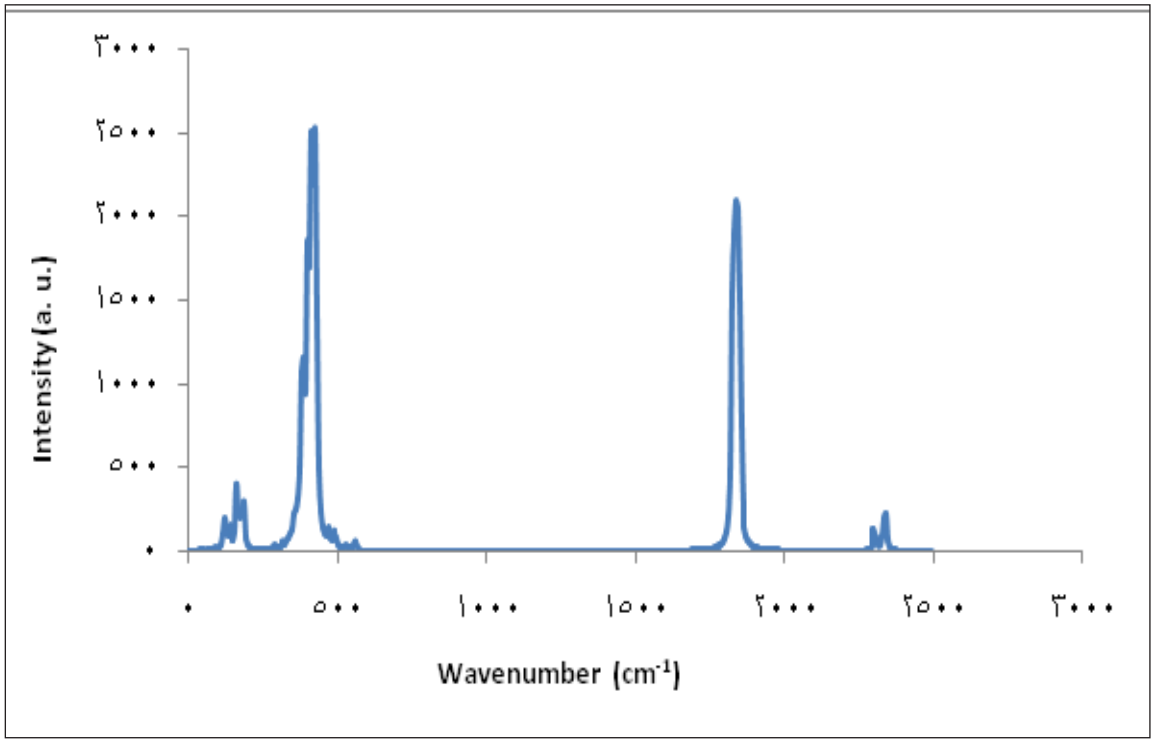

Fig. 8. IR spectrum of HP wurtzoid structure molecules.

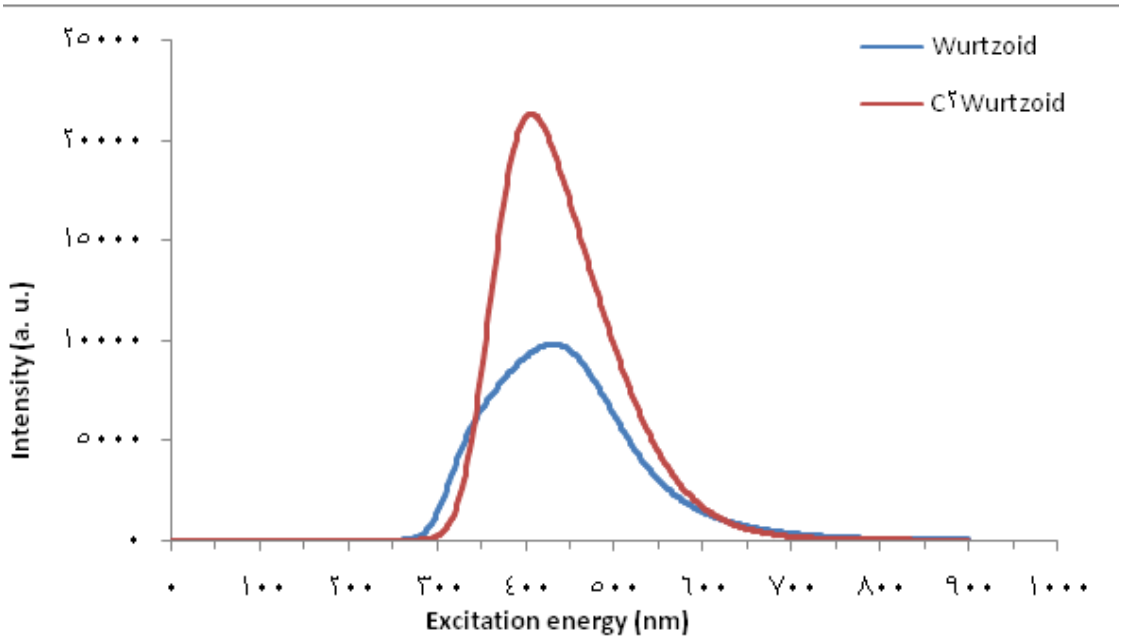

Fig. 9. UV-vis spectra of wurtzoid and wurtzoid2c structures.

Conclusions

The structural and vibrational properties of ZnnSen (n=1,3,7,13) nanostructures have been investigated by using wurtzoids structure, DFT/TDDFT at the B3LYP level with 6–311G basis functions and Gaussian 09 program. The calculation results are in high agreement with experimental values. The bond length decreased with the size of the nanostructures in good agreement with the published experimental results. The energy gap and binding energy increased with nanostructures size while the energy gap converged to 2.7 eV. UV-vis spectra for wurtzoid and wurtzoid2c changed with the size of the structure and covered all visible region. The maximum peak for wurtzoid at 430.2 nm is shifted to 405 nm for wurtzoid2c. Therefore, the optical properties can be modified to the desired values by reducing or expanding the size of nanostructures. This leads to wide applications in photoelectronic devices, lasers, sensors, and LEDs.

Conflicts of interest

The authors declare that they have no known competing financial interests or personal relationships that could have appeared to influence the work reported in this paper.

References

1. Ahmed H., Hashim A. and Abduljalil H. M., Analysis of Structural, Electrical and Electronic Properties of (Polymer Nanocomposites/ Silicon Carbide) for Antibacterial Application. *Egypt.J.Chem.* 62, 4. 1167 – 1176 (2019).

2. Hashim A. and Hadi Q., Synthesis of Novel (Polymer Blend-Ceramics) Nanocomposites: Structural, Optical and Electrical Properties for Humidity Sensors. *Journal of Inorganic and Organometallic Polymers and Materials*, 28, 4. 1394–1401 (2018).

3. Hashim A. and Hadi A., Novel Pressure Sensors Made From Nanocomposites (Biodegradable Polymers–Metal Oxide Nanoparticles): Fabrication And Characterization. *Ukrainian Journal of Physics*, 63, 8. (2018).

4. Gouma P. I., Nanomaterials for chemical sensors and biotechnology. *Pan Stanford Publishing Pte. Ltd*. (2010).

5. Ravindranadh K., Shekhawat M. S., and Rao M. C., Preparation and Applications of ZnSe Nanoparticles. *AIP Conf. Proc*. 1536, 219-220 (2013).

6. Yeh C.-Y., Lu Z. W., Froyen S., and Zunger A., Zinc-blende —wurtzite polytypism in semiconductors. *Physical Review* B 46, 1086-

1097 (1992).

7. Azpiroz J. M., Matxain J. M., Infante I., Lopez X., and Ugalde J. M., A DFT/TDDFT study on the optoelectronic properties of the amine-capped magic $(CdSe)_{13}$ nanocluster. *Physical Chemistry Chemical Physics* (2013).

8. Kumar D. S., Kashif M., Rethinasami V., Ravikumar B. , Pandiarajan S., Ayeshamariam A., Sivaranjani S., Bououdina M., and Ramalingam S., Synthesis and characterisation of zinc selenide (ZnSe) thin films electrodeposited on ITO and SnO_2 substrates. *Journal of Ovonic Research*, 10, 5. 175 – 184 (2014).

9. Boo B. H., Cho H.,and Kang D. E., Ab initio and DFT investigation of structures and energies of low-lying isomers of Zn_xSe_x (x = 1–4) clusters. *Journal of Molecular Structure: Theochem* 806, 77–83 (2007).

10. Makhavikou M., Parkhomenko I., Vlasukova L., Komarov F., Milchanin O., Mudryi A., Zhivulko V., Wendler E., Togambayeva A., and Korolik O., Raman monitoring of ZnSe and $ZnS_x Se_{1-x}$ nanocrystals formed in SiO_2 by ion implantation. *Nuclear Inst, and Methods in Physics Research* B(2018).

11. Yang C.S., Hsieh Y.P., Kuo M.C., Tseng P.Y., Yeh Z.W., Chiu K.C., Shen J.L., Chu A.H.M., Chou W.C., and Lan W.H., Compressive strain-induced heavy hole and light hole splitting of $Zn_{1-x}Cd_xSe$ epilayers grown by molecular beam epitaxy. *Materials Chemistry and Physics* 78, 602–607 (2003).

12. Hashim A., Abduljalil H. M., and Ahmed H., Fabrication and Characterization of $(PVA-TiO2)_{1-x}$/ SiC_x Nanocomposites for Biomedical Applications, *Egypt. J. Chem.,* DOI: 10.21608/EJCHEM.2019.10712.1695, (2019).

13. Ahmed H. and Hashim A., Fabrication of PVA/NiO/SiC Nanocomposites and Studying their Dielectric Properties For Antibacterial Applications, *Egypt. J. Chem.,* DOI: 10.21608/EJCHEM.2019.11109.1712, (2019).

14. Hashim A., Abduljalil H., and Ahmed H., Analysis of Optical, Electronic and Spectroscopic properties of (Biopolymer-SiC) Nanocomposites For Electronics Applications, *Egypt. J. Chem.,* DOI: 10.21608/EJCHEM.2019.7154.1590, (2019).

15. Jimenez-Izal E., Matxain J. M., Pirisab M., and Ugaldea J. M., Self-assembling endohedrally doped CdS nanoclusters: new porous solid phases of CdS. *Phys. Chem. Chem. Phys*. 14, 9676–9682 (2012).

16. Santhosh T.C.M., Bangera K. V. and Shivakumar G.K., Synthesis and bandgap tuning in $CdSe_{(1-x)}$ $Te_{(x)}$ thin films for solar cell applications. *Sol. Energy* 153, 343–347 (2017).

17. Saravanamoorthy S. N., Peter A. J. and Lee C. W., Optical peak gain in a PbSe/CdSe core-shell quantum dot in the presence of magnetic field for mid-infrared laser applications. *Chem. Phys*. 483–484 (2017).

18. Abed H. H., Abduljalil H. M., and Abdulsattar M. A., Structural, Optical and Humidity Sensitivity for CdSe Nanocrystalline Thin films. *J. Adv. Pharm. Edu. Res*. 8, 4. 52-31 (2018).

19. Sharma S., Malik M. A., Chandel T., Thakur V. and Rajaram P., Growth and Characterization of ZnSe Nanoparticles. *AIP Conf. Proc*. 1591, 474-476 (2014).

20. Deneuville A., Tanner D., and Hollo P.H., Optical constants of ZnSe in the far-infrared. *Physical review* B. 43, 8. (1991).

21. Abdulsattar M. A., GaN wurtzite nanocrystals approached using wurtzoids structures and their use as a hydrogen sensor: A DFT study. *Superlattices Microstruct*. 93, 163-170 (2016).

22. Abdulsattar M. A., Chlorine gas reaction with ZnO wurtzoid nanocrystals as a function of temperature: a DFT study. *J. Mol. Model*., 23, 125 (2017).

23. Abdulsattar M. A., Abduljalil H. M., and Abed H. H., Formation energies of CdSe wurtzoid and diamondoid clusters formed from Cd and Se atomic clusters. *Calphad*. 64, 37–42 (2019).

24. Abdulsattar M. A., Abduljalil H. M., and Abed H. H., Structure, Stability and Vibrational Properties of CdSe Wurtzite Molecules and Nanocrystals: A DFT Study. *Karbala International Journal of Modern Science*. 5, 119-125 (2019).

25. "Gaussian 09", Revision E.01, M. J. Frisch, G. W. Trucks, H. B. Schlegel, G. E. Scuseria, M. A. Robb, J. R. Cheeseman, G. Scalmani, V. Barone, B. Mennucci, G. A. Petersson, H Nakatsuji, M. Caricato, X. Li, H. P. Hratchian, A. F. Izmaylov, J. Bloino, G. Zheng, J. L. Sonnenberg, M. Hada, M. Ehara, K. Toyota, R. Fukuda, J. Hasegawa, M. Ishida, T. Nakajima, Y. Honda, O. Kitao, H. Nakai, T. Vreven, J. A. Montgomery, Jr, J. E. Peralta, F. Ogliaro, M. Bearpark, J. J. Heyd, E. Brothers,

K. N. Kudin, V. N. Staroverov, R. Kobayashi, J. Normand, K. Raghavachari, A. Rendell, J. C. Burant, S. S. Iyengar, J. Tomasi, M. Cossi, N. Rega, J. M. Millam, M. Klene, J. E. Knox, J. B. Cross, V. Bakken, C. Adamo, J. Jaramillo, R. Gomperts, R. E. Stratmann, O. Yazyev, A. J. Austin, R. Cammi, C. Pomelli, J. W. Ochterski, R. L. Martin, K. Morokuma, V. G. Zakrzewski, G. A. Voth, P. Salvador, J. J. Dannenberg, S. Dapprich, A. D. Daniels, €O. Farkas, J. B. Foresman, J. V. Ortiz, J. Cioslowski, and D. J. Fox, Gaussian, Inc., Wallingford CT, (2009) .

26. Kumar P., Singh J., Pandey M. K., Jeyanthi C.E., Siddheswaran R., Paulraj M., Hui K.N., and Hui K.S., Synthesis, structural, optical and Raman studies of pure and lanthanum doped ZnSe nanoparticles. Materials Research Bulletin. 49, 144–150 (2014).

الخصائص التركيبية ولأهتزازية للتراكيبZnSe النانوية: دراسة بأستخدام DFT/TDDFT

حسين حاكم عبد[١], محمد جاسم السلطاني[٢], مضر احمد عبد الستار[٣], حيدر محمد عبد الجليل[١]
[١]قسم الفيزياء, كلية العلوم,جامعة بابل,العراق.
[٢]قسم صحة البيئة, كلية علوم البيئة, جامعة القاسم الخضراء, العراق.
[٣]وزارة العلوم والتكنولوجيا, بغداد, العراق.

الخصائص التركيبية والأهتزازية للتراكيب النانوية (Zn_nSe_n (n=1,3,7,13 شخصت بواسطة برنامج الكاوسين ٠٩ وبأستخدام نظرية دالية الكثافة بشقيها المستقلة والمعتمدة على الزمن عند المستوي B3LYP مع دالة الأساس 6–311G. وقد أظهرت الخصائص التركيبية ان أعادة بناء ذرات السطح للبلورة يؤدي الى حدوث تغير في العديد من الأواصر ولأقتراب **من** حالتها المثالية عند الزيادة في حجم البلورة فطول الأصرة Zn-Se قل مع زيادة حجم التراكيب النانوية وأقتراب من القيمة المحسوبة تجريبيا لهذه الأصرة. كذلك لوحظ نقصان في التأثير الكمي لوحظ مع نمو الحجم للتراكيب النانوية: لذا فأن فجوة الطاقة تقترب من القيمة التجريبية ٢,٧ الكترون –فولت. علاوة على ذلك, طاقة الربط تزداد مع زيادة حجم التراكيب, كما هو الحال في بلورة وورتزايتc2 ($Zn_{13}Se_{13}$) تكون أكثر أستقرارية من التراكيب الصغيرة. نتائج الخصائص الأهتزازية تشير الى ان النمط البصري الطولي التجريبي (LO) متموضع بين النمط البصري النقي والمخمل بالهايدروجين ويكون قريب جدا من حالة النمط النقي, وهذا يعطي توافق جيد مع النتائج الموجودة تجريبيا. وجود ذرات الهايدروجين على السطح سبب نقصان مضاعف عدة مرات في ثابت القوة عن الحالة النقية. طيفIR للورتزويد ولورتزويد المخمل بالهايدروجين شخصت. الحافة البصرية في أطياف UV-vis للورتزويد تقل من ٤,٥ الكترون –فولت الى ٤,٢ الكترون- فولت للورتزويد c2 للزيادة في حجم التركيب النانوي, بينما أعلى قمة للورتزويد عند2.88 الكترون-فولت تزداد الى 3.06 الكترون-فولت للورتزويدc2 مضهرتا أزاحة واضحه نحو الأزرق. هذه النتائج تقود الى تطبيقات واسعة في عدة مجالات مثلا الأجهزه الضوئية –الكترونية والليزرات والمتحسسات ولدايودات الباعثه للضوء.